Analysis of dipolar interactions in trapped 2D Bose-Einstein condensates

Bachelor's Thesis

Written by *Alfred B. Hansen*

16.6.2021

Supervised by
Michele Burrello

University of Copenhagen

UNIVERSITY OF
COPENHAGEN

Name of Institute:	The Niels Bohr Institute
Name of Department:	Condensed Matter Theory
Author:	Alfred B. Hansen
Email:	jpg878@alumni.ku.dk

Title and subtitle:	Analysis of dipolar interactions in trapped 2D Bose-Einstein condensates
Supervisor:	Michele Burrello
Handed in:	16.6.2021
Defended:	24.6.2021

Abstract

In this thesis we will treat trapped ultra cold dipolar atomic gases, of which the study in recent years has intensified, showing great promises in exploring quantum phenomena. One such phenomenon is the simulation of Quantum Hall states. We will explore how trapped rotating dipolar gases provide us with better opportunities to reach the Quantum Hall regime, by introducing the long range repulsive dipolar interaction. The dipolar interaction lowers the filling factor of the system, to make it possible to reach the Quantum Hall regime for 3000 atoms under realistic conditions.

Contents

1 Introduction

Bose-Einstein condensates (BECs) were first realized by W. Ketterle, C. E. Wieman and E. A. Cornell in 1995, in ultra cold systems of alkali atoms, reaching temperatures on a micro-kelvin scale [1] and even down to 170 nK [2], receiving a Nobel prize in 2001 for their work [3].

When a dilute gas of bosons, which are atoms with integer spin, is cooled down, the ground state of the system will be occupied by a large fraction of the particles in the gas, and thus approximately all the bosons will be in the same quantum state [4]. This gives rise to interesting quantum behavior on mesoscopic scales, such as superfluidity and quantized vortices, which can be used to explore different quantum phenomena.

When working with BECs, one will need to cool and trap the gas, to create an environment suitable for the realization of the condensate. Both the cooling and trapping can be done by utilizing lasers and exploiting how these interact with atoms, as described in chapter 4 of [4]. In the process of trapping the condensate, the harmonic trapping potential can be made anisotropic, by increasing the relative strength of the potential along one axis. This in turn will flatten the gas, and effectively create a 2-dimensional (2D) system [5].

Another effect obtained by exploiting this interaction of lasers and atoms, is the 'stirring' of the sample, where the now 2D gas is rotated [6]. In the rotating frame we will see a synthetic B-field emerging from the act of rotating the sample, which will be illuminating, especially through the magnetic length, when describing the different states that the condensate can obtain. We stress that the B-field is purely synthetic, and that the atoms which makes up the condensate are not charged, but only that the dynamics of the system resembles that of a charged particle in a magnetic field.

Increasing the rotational frequency of the trap will at some point make it energetically favorable for vortices to be created, aligning themselves in a triangular lattice.

For rapidly rotating condensates, we expect the gas to enter the Lowest Landau Level (LLL) vortex lattice regime [7], where the single particle energy spectrum resembles that of the Landau levels of the Quantum Hall effect, being highly degenerate. At this point, the vortex lattice melts when a sufficiently low value of the so-called filling factor, the ratio between atom (n) and vortex (n_v) densities,

$$\nu = \frac{n}{n_v} = \frac{2\pi n\hbar}{B}$$

is reached, and the condensate should enter the so-called Quantum Hall (QH) regime [8] [9].

In the last few years there have been several experimental groups focusing on the study of trapped ultra cold atomic gases with dipolar interactions [10] [11] [12]. The dipolar interaction makes it difficult to reach the condensed state, but the realization of dipolar BECs has allowed for the study of phenomena that could not be seen before.

Creating condensates of dipolar atoms alters the properties of the gas, since it introduces long-range dipole-dipole interactions, as opposed to only the short-ranged contact interaction. Dipolar condensates could make it easier to reach the QH regime, because the dipole-dipole interaction should reduce the density of the gas, and thus the filling factor. It has been shown, that for rotating 2D gases with another long range interaction, namely Rydberg-dressing, the QH regime can be reached more easily [9]. Since Rydberg-dressing introduces a long-range interaction, we want to investigate if the same physics appear in dipolar BECs.

Because of the dipolar nature of the condensate, it is possible to align the magnetic moment of the atoms, by the use of an external magnetic field. Here we wish to align all the dipoles to point in the same direction, perpendicularly out of the 2D gas. Doing so makes the dipole interaction entirely repulsive, and so increases the interaction energy.

In the scenario of dipole-dipole interactions we introduce a parameter g' that describes the effective contact interaction, taking into account the increased interaction strength from the dipolar effects in the 2D gas with aligned magnetic moments.

For weak magnetic fields, before the onset of the LLL regime, the dipole-dipole interaction should, for strong enough interactions, spontaneously break translational invariance, as shown in [13]. We estimate at what effective interaction strength g_{SS} the translational invariance should break, based

on the so-called roton spectrum, and compare this to the optimal interaction strength g_o to enter the QH regime. This will be done by finding the Bogoliubov-spectrum of the ultra-cold 2D condensate, and estimating for when the roton-instability occurs.

By increasing the effective interaction via the dipole-dipole interaction, we shall see that the superfluid healing length ξ is decreased, and the Lindemann length l_{L}, describing the size of the quantum fluctuations of the vortices [9], is increased, effectively suppressing the LLL regime, thus making it easier to enter the QH regime, by lowering the rotation required to do so.

In this project we want to approximate the density profile of a rapidly rotating 2D BEC of the dipolar Dysprosium (Dy) and Erbium (Er) atoms, with magnetic moments assumed to be aligned and pointing perpendicularly out of the 2D condensate. This will be done by assuming a strong harmonic trap along the z-axis, and using both a Gaussian and Thomas-Fermi ansatz with the purpose of minimizing the Gross-Pitaevskii (GP) energy when dipole-dipole interactions are considered. To this end we will adopt a mean-field approach using the Gross-Pitaevskii equation (GPE) to describe the behavior of the condensate. When the distribution has been determined the density and also the filling factor can be found, and from this the rotation required to enter the QH regime can be determined.

2 The physics of BECs

The physics of BECs are typically described by using a mean-field approach resulting in the GPE, which is analogous to the Schrodinger equation but for a many-particle quantum system at zero-temperature. It is a mean-field approach, characterized by assuming that all the particle are in the ground state, and that the many-body wave function can be expressed as the product of all the single-particle wave functions, neglecting higher-order correlations. This amounts to replacing the real potential between atoms with a more simple and approximate potential, namely the contact interaction [14]. When two particles are near each other, the contact interaction can be described by $g\delta(\mathbf{r}-\mathbf{r}')$ where $g = 4\pi\hbar^2 a/m$ and a is the scattering length, measuring how much the wave function of a particle is affected by another. This is done since it is computationally unrealistic to calculate the individual interactions of thousands of particles. In the BEC all the particles are in the same single particle state $\phi(\mathbf{r})$, normalized to 1, so it is assumed that the many-body wave function can be expressed as

$$\Psi(\mathbf{r}_1, ..., \mathbf{r}_N) = \prod_{i=1}^{N} \phi(\mathbf{r}_i) \tag{1}$$

For the mean-field regime to hold, we expect the fraction of particles in the ground state to be very large. The depletion d of the BEC, being the fraction of particles not in the ground state, scales like $d \propto (a/r_s)^{3/2}$, where r_s is the interatomic length. These atoms not in the ground state are due to correlations at small r_s that the mean-field approach discards [4]. Therefore d is a good measure of when the mean-field approach is valid, and we expect the size of the depletion to be negligible.

Since there are N particles in the condensate, one defines the wave function of the condensate

$$\psi(\mathbf{r}) = N^{1/2}\phi(\mathbf{r}) \tag{2}$$

Which, as we will see, gives a convenient normalization

$$\int |\psi(\mathbf{r})|^2 \, \mathrm{d}\mathbf{r} = \int N|\phi(\mathbf{r})|^2 \, \mathrm{d}\mathbf{r} = N \tag{3}$$

With this in place the basic GPE can be formulated

2.1 Non-rotating BEC

To describe the BEC, we assume an external potential $V(\mathbf{r})$ trapping the gas, and so the Hamiltonian describing all the particles will consist of the kinetic and potential energies of all the single particle states and an interaction term [4], such that

$$H = \sum_{i=1}^{N} \left[\frac{\mathbf{p}_i^2}{2m} + V(\mathbf{r}_i) \right] + g \sum_{k<l}^{N} \delta(\mathbf{r}_k - \mathbf{r}_l) \tag{4}$$

Where the momentum operator in position space is given as $\mathbf{p}_i = \frac{\hbar}{i} \frac{\partial}{\partial x_i}$. In the last term the sum runs over $k < l$ as to not double-count interactions. The energy of the system is then

$$E[\phi] = \int \mathrm{d}\mathbf{r}_1 ... \, \mathrm{d}\mathbf{r}_N \prod_{i=1}^{N} \phi^*(\mathbf{r}_i) \left(\sum_{i=1}^{N} \left[\frac{\mathbf{p}_i^2}{2m} + V(\mathbf{r}_i) \right] + g \sum_{k<l}^{N} \delta(\mathbf{r}_k - \mathbf{r}_l) \right) \prod_{i=1}^{N} \phi(\mathbf{r}_i) \tag{5}$$

$$= \sum_{i}^{N} \left(\int \mathrm{d}\mathbf{r}_i \phi_i^* \left[\frac{\mathbf{p}_i^2}{2m} + V(\mathbf{r}_i) \right] \phi_i \prod_{j \neq i}^{N} \int \mathrm{d}\mathbf{r}_j \, |\phi(\mathbf{r}_j)|^2 \right) + \int \mathrm{d}\mathbf{r}_1 ... \, \mathrm{d}\mathbf{r}_N \prod_{i=1}^{N} \phi^*(\mathbf{r}_i) \left(g \sum_{k<l}^{N} \delta(\mathbf{r}_k - \mathbf{r}_l) \right) \prod_{i=1}^{N} \phi(\mathbf{r}_i) \tag{6}$$

The last term can be seen as choosing the upper triangular part of the interaction matrix excluding the diagonal, which has $\frac{N(N-1)}{2}$ terms, correlating two particles giving a $|\phi(\mathbf{r})|^4$ term since it takes the indices k and l, and lets $k = l$. The term $\prod_{j \neq i}^{N} \int \mathrm{d}\mathbf{r}_j \, |\phi(\mathbf{r}_j)|^2 = 1$ because of the normalization of the single particle wave function. This results in an energy-functional of the system given as

$$\begin{aligned} E[\phi] &= \sum_{i}^{N} \int \mathrm{d}\mathbf{r}_i \phi_i^* \left[\frac{\mathbf{p}_i^2}{2m} + V(\mathbf{r}_i) \right] \phi_i \cdot 1 + \int \mathrm{d}\mathbf{r} \frac{N(N-1)}{2} g |\phi(\mathbf{r})|^4 \\ &= N \int \mathrm{d}\mathbf{r} \phi^*(\mathbf{r}) \frac{-\hbar^2}{2m} \nabla^2 \phi(\mathbf{r}) + V(\mathbf{r}) |\phi(\mathbf{r})|^2 + \frac{(N-1)}{2} g |\phi(\mathbf{r})|^4 \end{aligned} \tag{7}$$

Doing an integration by parts on the first term, demanding that the single particle wave function vanishes far away, on gets

$$E[\phi] = N \int \mathrm{d}\mathbf{r} \, \frac{\hbar^2}{2m} |\nabla \phi(\mathbf{r})|^2 + V(\mathbf{r}) |\phi(\mathbf{r})|^2 + \frac{(N-1)}{2} g |\phi(\mathbf{r})|^4 \tag{8}$$

Here the normalization from Eq. (3) comes in handy, giving

$$E[\psi] = \int \mathrm{d}\mathbf{r} \, \frac{\hbar^2}{2m} |\nabla \psi(\mathbf{r})|^2 + V(\mathbf{r}) |\psi(\mathbf{r})|^2 + \frac{1}{2} g |\psi(\mathbf{r})|^4 - \frac{1}{2N} g |\psi(\mathbf{r})|^4 \tag{9}$$

Assuming $N >> 1$, the last term is negligible because of the factor $1/N$

$$E[\psi] = \int \mathrm{d}\mathbf{r} \, \frac{\hbar^2}{2m} |\nabla \psi(\mathbf{r})|^2 + V(\mathbf{r}) |\psi(\mathbf{r})|^2 + \frac{1}{2} g |\psi(\mathbf{r})|^4 \tag{10}$$

Using a variational approach, letting $\psi^* \to \psi^* + \delta\psi^*$, where $\delta\psi^*$ is a small change in ψ^*, imposing the demand that $\delta E = E[\psi, \psi^* + \delta\psi^*] - E[\psi, \psi^*] = \mu \delta N$, and throwing away all second order variations, the energy-functional can be minimized. Here μ is the chemical potential, acting like a Lagrange multiplier, making sure that the number of particles remains constant. Not including the second order variations arising from $|\psi(\mathbf{r})|^4$, the variation is

$$\delta E = \int \mathrm{d}\mathbf{r} \, \frac{\hbar^2}{2m} (\nabla \psi^* \nabla \psi + \nabla \delta\psi^* \nabla \psi) + V(\mathbf{r})(\psi^* \psi + \delta\psi^* \psi) + \frac{1}{2} g((\psi^* \psi)^2 + 2\psi^* \psi \delta\psi^* \psi) - E[\psi, \psi^*]$$

$$= \int \mathrm{d}\mathbf{r} \, \frac{\hbar^2}{2m} (\nabla \delta\psi^* \nabla \psi) + V(\mathbf{r})(\delta\psi^* \psi) + g|\psi|^2 \psi \delta\psi^* \tag{11}$$

Integrating the first term by parts to rewrite the integrand to be linear in $\delta\psi^*$

$$\delta E = \int \mathrm{d}\mathbf{r} \left[\frac{-\hbar^2}{2m}\nabla^2\psi + V(\mathbf{r})\psi + g|\psi|^2\psi \right] \delta\psi^* \tag{12}$$

The variation $\mu\delta N$ is found as

$$\delta N = \int \mathrm{d}\mathbf{r}\, \psi^*\psi + \delta\psi^*\psi - |\psi|^2 = \int \mathrm{d}\mathbf{r}\, \delta\psi^*\psi \tag{13}$$

And so, since demanding that $\delta E = \mu\delta N$ has to hold true for all arbitrary variations $\delta\psi^*$, the integrands can be equated and one obtains the GPE

$$\frac{-\hbar^2}{2m}\nabla^2\psi + V(\mathbf{r})\psi + g|\psi|^2\psi = \mu\psi \tag{14}$$

The primary difference, and as we shall see difficulty, between the GPE and Schrödinger equation is that we have a non-linear mean-field term $g|\psi|^2\psi$, due to the particle interaction. Another notable difference is that the left hand side of Eq. (14) does not equal the energy of the system, but the energy per particle μ.

2.2 Trapping of the BEC

When working with BECs one will often use some form of trapping to contain and manipulate the gas. Here we will describe a condensate in harmonic trap, induced by the interaction between lasers and atoms, as in chapter 4 of [4]. This results in a harmonic trap along the z-axis that can be described by the potential $V(\mathbf{r}) = \frac{1}{2}m\omega_z^2 z^2 + V_{2D}(x, y)$. The regime at interest is for weak interactions, that is $g|\psi|^2 << \hbar\omega_z$, and the trap will be anisotropic such that the potential is strongest along the z-axis. This will result in the condensate becoming effectively 2D, or quasi-2D, confined in the ground state of the trap in the z-direction [5].

By plugging the potential into Eq. 10 one could go through the variational calculation once again to obtain the equations of motion. We instead opt to use a trial-wave method, where an ansatz is proposed with a suitable variational parameter, which will be determined by minimizing the energy of Eq. 10. A reasonable ansatz would be a Gaussian density distribution, since this is the solution to the harmonic potential. Assuming separability of the wave function, such that $\psi(\mathbf{r}) = \phi(z)\chi(x, y)$, the ansatz is chosen as

$$\phi(z) = \frac{e^{-z^2/2\eta^2}}{\sqrt{\eta\sqrt{\pi}}} \tag{15}$$

Where η is the variational parameter. Following the method laid out in [5], by integrating out the z-dependence in Eq. 10 and using the Euler-Lagrange equations to minimize the functional, it is shown that $\eta = a_z$ in the limit of weak interactions. Here $a_z = \sqrt{\hbar/m\omega_z}$ is the length of oscillations in the z-direction. From this, in the stationary case, the effectively 2D GPE becomes

$$\chi(x, y)\mu = \left[\frac{-\hbar^2}{2m}\nabla_\perp^2 + V(x, y) + \frac{g}{\sqrt{2\pi}a_z}|\chi(x, y)|^2 \right] \chi(x, y) \tag{16}$$

Where $\nabla_\perp^2$ is the Laplacian in the xy-plane. In our case, we also want to apply a harmonic potential in the x- and y-direction, but with the same frequency Ω_{tr}, where $\Omega_{tr} << \omega_z$, such that

$$V(x, y) = \frac{1}{2}m\Omega_{tr}^2(x^2 + y^2) = \frac{1}{2}m\Omega_{tr}^2\rho^2\,, \quad \rho^2 = x^2 + y^2 \tag{17}$$

Now one can go about rotating the sample.

2.3 Rotation of the BEC

When rotating the sample, the description will most easily be done in that of the rotating frame. Therefore one applies the unitary rotation operator to the Hamiltonian describing the system. Here it is import to consider the time-dependent GPE, since the rotation is indeed a dynamical phenomenon. The rotation operator, assuming that the rotation is around the z-axis, such that the angular momentum is only along the z-axis, is [15]

$$R(t) = e^{-i\phi(t)L_z/\hbar} = e^{-i\Omega_{rot}tL_z/\hbar} \tag{18}$$

This is a unitary operator i.e. $R^\dagger R = 1$ and so the time-dependent GPE can be transformed to a rotated frame, as done in Appendix C, where

$$H_{Rot} = H - \Omega_{rot}L_z \tag{19}$$

Therefore the kinetic and harmonic potential term of the 2D Hamiltonian in the rotated frame can be expressed as

$$H_{Rot} = \frac{\mathbf{p}^2}{2m} - \Omega_{rot}L_z + \frac{1}{2}m\Omega_{tr}^2\rho^2 \tag{20}$$

An effective vector potential $\mathbf{A}$ can be used to simplify above equation, and rewrite the Hamiltonian as to resemble that of a charged particle in a magnetic field produced by the vector potential $\mathbf{A} = \Omega_{rot}m(y, -x)$. We stress that it is only the mathematical description that has this resemblance, and that there is not an actual magnetic field nor any charges present. From $\mathbf{A}$ we see that the synthetic magnet field has the form $B = 2m\Omega_{rot}$. Using that $L_z = (\mathbf{r} \times \mathbf{p})_z = (xp_y - yp_x)$ the following relation is obtained

$$\frac{(\mathbf{p} + \mathbf{A})^2}{2m} = \frac{\mathbf{p}^2}{2m} + \frac{\mathbf{A}^2}{2m} + \frac{2m\Omega_{rot}}{2m}(yp_x - xp_y) \tag{21}$$

$$= \frac{\mathbf{p}^2}{2m} + \frac{\Omega_{rot}^2 m}{2}\rho^2 - \Omega_{rot}L_z \tag{22}$$

And so we see that

$$\frac{(\mathbf{p} + \mathbf{A})^2}{2m} - \frac{\Omega_{rot}^2 m}{2}\rho^2 = \frac{\mathbf{p}^2}{2m} + \frac{\Omega_{rot}^2 m}{2}\rho^2 - \Omega_{rot}L_z \tag{23}$$

Thus the Hamiltonian in the rotating frame can be rewritten in terms of the vector potential as

$$H_{Rot} = \frac{(\mathbf{p} + \mathbf{A})^2}{2m} - \frac{\Omega_{rot}^2 m}{2}\rho^2 + \frac{1}{2}m\Omega_{tr}^2\rho^2$$

$$= \frac{(\mathbf{p} + \mathbf{A})^2}{2m} + \frac{1}{2}m\Omega_{tr}^2(1 - \gamma^2)\rho^2 \tag{24}$$

We see that the first term of the Hamiltonian is that of a particle in a magnetic field produced by $\mathbf{A}$. Here $\gamma = \Omega_{rot}/\Omega_{tr}$ will be an important parameter, describing the ratio of the rotational frequency of the sample and the frequency of the harmonic trap. When Ω_{rot} becomes bigger than Ω_{tr}, the potential term becomes negative, indicating that the sample is rotating so fast as to be ripped apart, which can be understood through the centripetal forces arising from the rotation, as visualized in Figure 1. This also sets a hard boundary of the rotational frequencies on can reach.

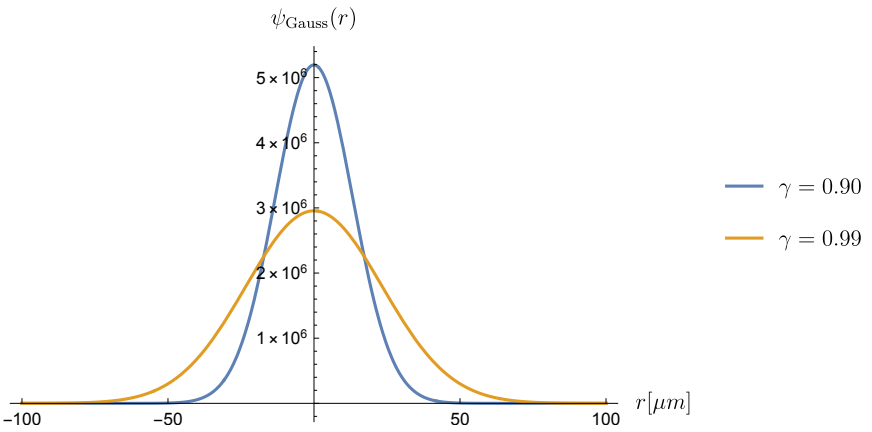

Figure 1: The effects of γ on a Gaussian profile. A bigger γ spreds out the distribution.

At some point, when the condensate is rotated fast enough, it will be energetically favorable for vortices to be nucleated in the 2D condensate [8], adding a quantum of rotation for each atom, since the superfluid nature of the condensate means that it will not rotate as a normal fluid. As we can see from Eq. 19, adding angular momentum will lower the energy. For a rapidly rotating sample, the areal density of vortices is proportional to the rotational frequency

$$n_v = \frac{m\Omega_{rot}}{\pi\hbar} = \frac{B}{2\pi\hbar} \tag{25}$$

We also observe that, when $\gamma \approx 1$ the harmonic potential in the xy-plane disappears and we are left with a Hamiltonian which resembles that of a particle in a magnetic field, which gives rise to the Quantum Hall effect, where the particle states are almost degenerate. In this scenario, the single particle states are that of the lowest Landau level to a good approximation, and we are thus in the LLL regime [7].

From (25) we see that the inter-vortex distance in the LLL vortex lattice, proportional to $\sqrt{1/n_v}$, scales like the so-called magnetic length $l_{\text{B}} = \sqrt{\hbar/B}$. We also note that in the the LLL vortex lattice, the core size of the vortices also scale with l_{B} [7].

When considering a vortex lattice, we have to introduce a modulation of the wave function to make sure that it vanishes in the vortices but that it is still, in our case, a Gaussian or Thomas-Fermi distribution overall, also called an envelope, as seen in Figure 2.

As shown in [9], if one introduces the vortex lattice, the modulation one has to make to the wave function cancels the effects of the vector potential $\mathbf{A}$. On the other hand the modulation enhances the contact interaction, since they find that the contribution from the modulation to the contact interaction term is $\int d\mathbf{r}\,|p(\mathbf{r})|^4 = b \approx 1.1596$. Here $p(\mathbf{r})$ is the modulation one has to multiply with the envelope to obtain the full vortex lattice wave function, with normalization $A^{-1}\int d\mathbf{r}\,|p(\mathbf{r})|^2 = 1$, where A is the area of a triangular vortex lattice unit cell $2\pi\hbar/B$ in the LLL regime. This approximation can be made if one assumes that $s >> l_{\text{B}}$, where s is the radial size of the condensate, since within a unit cell the density, harmonic potential and other interactions can be assumed to be constant [16].

Considering all the above, the Hamiltonian describing the vortex lattice in the quasi-2D regime can be expressed

$$H = \frac{\mathbf{p}^2}{2m} + \frac{1}{2}m\Omega_{tr}^2(1-\gamma^2)\rho^2 + \frac{gb}{\sqrt{2\pi}a_z}|\chi(\boldsymbol{\rho})|^2 \tag{26}$$

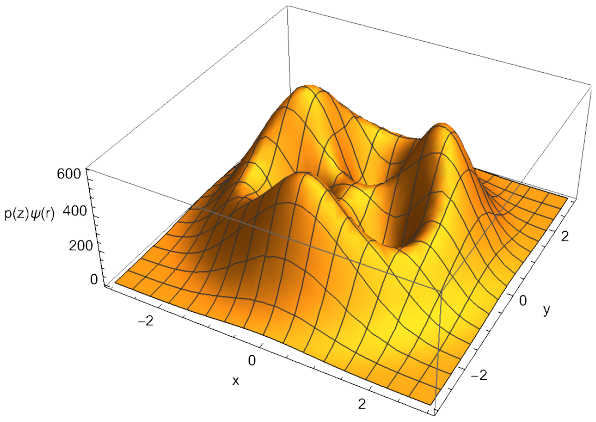

Figure 2: Schematic density of a Gaussian envelope with three vortices, produced by the modulation $p(z) = \prod_i (z - \eta_i)$ where $z = x + iy$ and η_i is the complex coordinates of the i'th vortex [9]. We assume that there are many vortices and that $s >> l_{\mathrm{B}}$, meaning that the radius of the condensate is much bigger than the inter-vortex distance, and thus stress that this is only a schematic depiction.

2.4 Dipolar BECs

Now we turn to the dipole-dipole interaction which is a main component of the setup, since the goal is to estimate if such an interaction can get the condensate closer to the QH regime. The energy from the dipole-dipole interaction where the dipoles are polarized in the same direction is highly anisotropic and given as [14]

$$U_{dd}(\mathbf{r}) = \frac{C_{dd}}{4\pi} \frac{1 - 3\cos^2(\theta)}{|\mathbf{r}|^3} \tag{27}$$

Where θ is the angle between the direction of the polarization and a straight line connecting two dipoles, $\mathbf{r}$ is the distance between two dipoles and C_{dd} is the strength of the interaction. This can be reformulated as [17]

$$U_{dd}(\mathbf{r}) = -C_{dd} \left[\frac{1}{3}\delta(\mathbf{r}) + \partial_{\mathbf{nn}} \frac{1}{4\pi|\mathbf{r}|} \right] \tag{28}$$

Where $\partial_{\mathbf{n}} = \mathbf{n} \cdot \nabla$ and so $\partial_{\mathbf{nn}} = \partial_{\mathbf{n}}(\partial_{\mathbf{n}})$. From Eq. (28) it is clear that the dipole-dipole interaction has both a short-range term coming from $\delta(\mathbf{r})$ and a long-range interaction $\partial_{\mathbf{nn}} \frac{1}{|\mathbf{r}|}$. The energy from the dipole-dipole interaction adds a term to the 3D GPE energy, given as

$$\int \mathrm{d}\mathbf{r}' \psi^*(\mathbf{r}') U_{dd}(\mathbf{r} - \mathbf{r}') \psi(\mathbf{r}')$$

$$= -\frac{C_{dd}}{3}|\psi(\mathbf{r})|^2 - C_{dd}\partial_{\mathbf{nn}} \int \mathrm{d}\mathbf{r}' U_{3D}(\mathbf{r} - \mathbf{r}')|\psi(\mathbf{r}')|^2 = -\frac{C_{dd}}{3}|\psi(\mathbf{r})|^2 + \Phi(\mathbf{r}) \tag{29}$$

Where $U_{3D}(\mathbf{r}) = \frac{1}{4\pi|\mathbf{r}|}$ and $\Phi(\mathbf{r}) = -C_{dd}\partial_{\mathbf{nn}} \int \mathrm{d}\mathbf{r}' U_{3D}(\mathbf{r} - \mathbf{r}')|\psi(\mathbf{r}')|^2$, so before reducing to the quasi-2D form, the GPE reads

$$-\frac{\hbar}{i}\partial_t \psi(\mathbf{r}) = \left[\frac{\mathbf{p}^2}{2m} + \frac{1}{2}m\omega_z^2 z + \frac{1}{2}m\Omega_{tr}^2(1 - \gamma^2)\rho^2 + b\left(g - \frac{C_{dd}}{3}\right)|\psi(\mathbf{r})|^2 + \Phi(\mathbf{r}) \right] \psi(\mathbf{r}) \tag{30}$$

The contact interaction from the dipoles also gets multiplied by b from the lattice modulation since it has the the same functional form. The dipole-dipole interaction lowers the effective contact interaction in 3D, when all the dipoles are polarized along the same axis. This is because dipoles

are attracted to each other when they are aligned head to tail and repulsed when side by side. As we shall see, the contribution to the contact interaction from the dipole-dipole term is positive when in the quasi-2D regime.

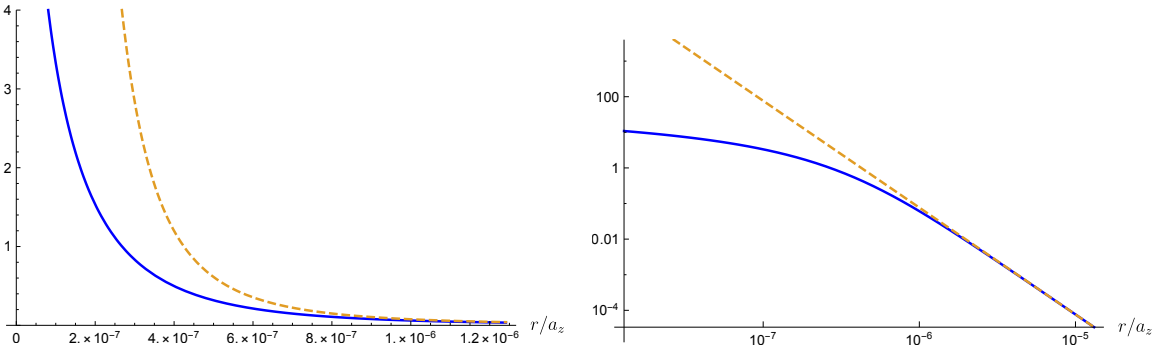

(a) Linear scale **(b)** Loglog scale

Figure 3: Here $-U(r)$ (solid blue) and $2\sqrt{2\pi}r^{-3}$ (dashed red) are plotted both for a normal (a) and a loglog (b) scale. Without trapping the BCE the dipolar interaction energy is proportional to r^{-3} as seen in Eq (27), but the interaction energy changes due to the trapping. At large distances the 2D effects should not be visible so we expect the two potentials to look the same, and so the factor $2\sqrt{2\pi}$ ensures that $-U(r)$ and $2\sqrt{2\pi}r^{-3}$ converges at the same asymptote for large r.

Following that of [18] one can now do as in Section 2.2 where one assumes weak interaction, such that $\eta = a_z$, and that $\Phi(r) << \hbar\omega_z$ and $\tilde{g}|\psi(r)|^2 << \hbar\omega_z$, where $\tilde{g}$ is just a general contact interaction, and finally that $\Omega_{tr} << \omega_z$. The last three constraints are made to make sure that the condensate is in the ground state of the harmonic trap along z and thus in a quasi-2D regime, since all energy scales are very low compared to that of the harmonic trap in the z-direction under these aforementioned constraints. The z-dependence is then integrated out, by assuming a Gaussian distribution along z. The first 4 terms in Eq. (30) are easily computed, since they are Gaussian integrals, but the long-range dipole-dipole term is rather tricky, and results in an effective long-range 2D dipole-dipole interaction

$$\Phi_{2D} = -C_{dd}\int \mathrm{d}\boldsymbol{\rho}'\, U(\boldsymbol{\rho}-\boldsymbol{\rho}')|\psi(\boldsymbol{\rho}')|^2 \tag{31}$$

Where the kernel $U(\boldsymbol{\rho})$ for polarization along the z-axis [18] is

$$U(\boldsymbol{\rho}) = \frac{1}{2(2\pi)^{3/2}a_z^3}e^{\boldsymbol{\rho}^2/4a_z^2}\left[-\left(2+\frac{\boldsymbol{\rho}^2}{a_z^2}\right)K_0\left(\frac{\boldsymbol{\rho}^2}{4a_z^2}\right)+\frac{\boldsymbol{\rho}^2}{a_z^2}K_1\left(\frac{\boldsymbol{\rho}^2}{4a_z^2}\right)\right], \tag{32}$$

Here K_0 and K_1 are the modified Bessel functions of the second kind, of order 0 and 1 respectively. This potential is modified from the r^{-3} potential that one sees in 3D, as shown in Figure 3. The GP energy in the quasi-2D regime with dipole-dipole interaction is then

$$E[\psi(\boldsymbol{\rho})] = \int d\boldsymbol{\rho}\left[-\psi(\boldsymbol{\rho})^*\frac{\hbar^2}{2m}\nabla^2\psi(\boldsymbol{\rho})+\frac{1}{2}m\Omega_{tr}^2(1-\gamma^2)\boldsymbol{\rho}^2|\psi(\boldsymbol{\rho})|^2+\frac{1}{2}b\tilde{g}|\psi(\boldsymbol{\rho})|^4+\Phi_{2D}|\psi(\boldsymbol{\rho})|^2\right] \tag{33}$$

Here

$$\tilde{g} = \frac{1}{a_z\sqrt{2\pi}}\left(g + \frac{2}{3}C_{dd}\right) \tag{34}$$

And $\psi(\boldsymbol{\rho})$ is the 2D wave function. As mentioned, the contribution to the contact interaction from the dipole-dipole term is positive, since the dipoles now only can lay besides each other and point in the same direction, thus only interacting repulsively.

3 Density distribution

The energy functional for the system has been determined as Eq. (33) and the density distribution, or more precisely the envelope, of the condensate can now be estimated. This is done by picking a suitable ansatz or trial wave function with a variational parameter, and minimizing the energy with respect to said parameter. Here both a Gaussian and Thomas-Fermi distribution is considered. The Gaussian since it is the solution to the harmonic potential that is assumed in the xy-plane, without the contact interaction term, and the Thomas-Fermi since it is the solution to the GPE when the kinetic energy is neglected, since the system is assumed to be dominated by the contact interaction.

The distribution will thus not be the exact ground state of the system, but rather a distribution that minimizes the energy for either a Gaussian or Thomas-Fermi shape. The exact ground state will likely be somewhere in between the two shapes.

3.1 Gaussian ansatz

The Gaussian ansatz for the envelope with variational parameter s is assumed to be of the form

$$\psi(x,y) = e^{-\frac{x^2+y^2}{2s^2}}\sqrt{\frac{N}{\pi s^2}} \tag{35}$$

Which is normalized to N, the number of atoms in the gas. The energy of the system is determined by Eq. (33) and the Laplacian of Eq. (35) is found since it is needed in the kinetic term. The ansatz has no angular dependence so the Laplacian of the Gaussian envelope in polar coordinates with radius ρ is

$$\nabla^2\psi(\rho) = \frac{1}{\rho}\partial_\rho\left(\rho\partial_\rho\psi(\boldsymbol{\rho})\right) = \psi(\rho)\left(\frac{\rho^2}{s^4} - \frac{2}{s^2}\right) \tag{36}$$

The energy from the first 3 terms in Eq. (33) is obtained by integrating over all space in polar coordinates, noting that $|\psi(\rho)|^2 = \psi(\rho)^2$ and remembering a factor 2π from the angular integral

$$2\pi\int_0^\infty \mathrm{d}\rho\,\rho\left[\frac{-\hbar^2}{2m}\psi(\rho)^2\left(\frac{\rho^2}{s^4} - \frac{2}{s^2}\right) + \frac{1}{2}m\Omega_{tr}^2(1-\gamma^2)\rho^2\psi(\rho)^2 + \frac{1}{2}b\tilde{g}\psi(\rho)^4\right] \tag{37}$$

$$= \frac{N\hbar^2}{2ms^2} + \frac{Nm\Omega_{tr}^2(1-\gamma^2)s^2}{2} + \frac{\tilde{g}bN^2}{4\pi s^2} \tag{38}$$

Finding the energy contribution from the Φ_{2D} term, we write out the energy from the term using Eq. (31)

$$E_{\Phi 2\mathrm{D}} = \langle\Phi_{2D}\rangle = -C_{dd}\frac{N^2}{\pi^2 s^4}\int dx'dy'dx\,dy\,e^{-(x^2+y^2+x'^2+y'^2)/s^2}U(x-x',y-y') \tag{39}$$

Shifting to the center of mass ρ_{cm} and relative coordinates ρ_{rel} as shown in Appendix A, one gets

$$E_{\Phi 2\mathrm{D}} = -C_{dd}\frac{4N^2}{s^4}\int_0^\infty\int_0^\infty \mathrm{d}\rho_{cm}\,d\rho_{rel}\,e^{-2\rho_{cm}^2/s^2}e^{-\rho_{rel}^2/2s^2}U(\rho_{rel})\rho_{cm}\rho_{rel} \tag{40}$$

The ρ_{cm} integral can now be done, and yields

$$E_{\Phi 2D} = -C_{dd}\frac{4N^2}{s^4}\frac{s^2}{4}\int_0^\infty \mathrm{d}\rho_{rel}\, e^{-\rho_{rel}^2/2s^2}U(\rho_{rel})\rho_{rel} \tag{41}$$

The substitution $\rho_s = \rho_{rel}/s$ is done such that the expression becomes

$$E_{\Phi 2D} = -C_{dd}\frac{N^2}{s^2}\int_0^\infty \mathrm{d}\rho_s\, e^{-\rho_s^2/2}U(\rho_s)\rho s^2 = -C_{dd}N^2\int_0^\infty d\rho_s\, e^{-\rho_s^2/2}U(\rho_s)\rho_s \tag{42}$$

Where now the kernel of the long-range dipole-dipole interaction is rewritten as

$$U(\rho_s) = \frac{1}{2(2\pi)^{3/2}a_z^3}e^{\rho_s^2 s^2/4a_z^2}\left[-\left(2+\frac{\rho_s^2 s^2}{a_z^2}\right)K_0\left(\frac{\rho_s^2 s^2}{4a_z^2}\right)+\frac{\rho_s^2 s^2}{a_z^2}K_1\left(\frac{\rho_s^2 s^2}{4a_z^2}\right)\right] \tag{43}$$

This integral converges and when the limit $s/a_z >> 1$ is considered to leading order, the energy becomes

$$E_{\Phi 2D} \approx C\frac{4a_z^2}{s^2} \tag{44}$$

Where $C = \frac{1}{2(2\pi)^{3/2}a_z^3}C_{dd}N^2$. Therefore the energy of the Gaussian distribution to leading order in s is

$$E = \frac{N\hbar^2}{2ms^2} + \frac{Nm\Omega_{tr}^2(1-\gamma^2)s^2}{2} + \frac{\tilde{g}bN^2}{4\pi s^2} + C\frac{4a_z^2}{s^2} \tag{45}$$

To determine the variational parameter s, the condition that $\frac{\partial E}{\partial s} = 0$ is imposed which yields

$$\frac{-N\hbar^2}{ms^3} + Nm\Omega^2(1-\gamma^2)s - \frac{\tilde{g}bN^2}{2\pi s^3} - C\frac{8a_z^2}{s^3} = 0 \tag{46}$$

Solving this gives an expression for the variational parameter for the Gaussian envelope

$$s_{\mathrm{Gauss}} = \sqrt[4]{\frac{2\pi\hbar^2 + Nmg'_{\mathrm{Gauss}}}{2\pi m^2\Omega_{tr}^2(1-\gamma^2)}} \tag{47}$$

For which

$$g'_{\mathrm{Gauss}} = b\tilde{g} + \frac{2^{3/2}C_{dd}}{\sqrt{\pi}a_z} \approx 0.46\frac{g}{a_z} + 1.9\frac{C_{dd}}{a_z} \tag{48}$$

To determine the uniform density of the 2D condensate, when assuming a Gaussian distribution, we must consider how to determine the radius of the condensate. The Gaussian distribution has no defined radius, as opposed to the Thomas-Fermi, so the radius must be approximated. The radius must not be too big, such that the density becomes too small, since we then cannot assure that the gas is til in the BEC state. The radius must also be small enough, such that assuming a uniform density can be an appropriate estimate. We adopt the convention of a radius of $2s_{Gauss}$, such that an approximate uniform density is $N/4\pi s_{Gauss}^2$.

We propose that one could refine this estimate by considering different expectation values obtained from the Gaussian. However, we note that $\langle\rho^2\rangle = s_{Gauss}^2$ which we estimate is too small to be used instead of $4s_{Gauss}^2$.

3.2 Thomas-Fermi ansatz

For the Thomas-Fermi ansatz, taking the shape of an inverted parabola, the envelope in the xy-plane, with radial polar coordinate ρ is chosen to be

$$\psi(\rho) = \sqrt{\frac{2N}{(2s)^2\pi}\left(1-\frac{\rho^2}{(2s)^2}\right)} \quad , \quad \rho < 2s \tag{49}$$

This distribution has a definite radius, as opposed to the Gaussian distribution, here chosen to be $2s$. The radius is chosen as $2s$ such that it can more readily be compared to the Gaussian ansatz. The reason for choice of the Thomas-Fermi ansatz originates from discarding the kinetic interaction in Eq. (14), such that the density can be expressed as

$$|\psi| = \sqrt{\frac{\mu - V}{g}} \tag{50}$$

This motivates the ansatz, as one can see by plugging in a harmonic potential. It is also evident that there must be some radius for which the wave function is 0, determined by when $\mu = V$ since $|\psi|$ must be real. If the kinetic term is negligible, it is reasonable to assume that this ansatz might perform well when the dipole-dipole interaction is introduced. Using Eq. (33) for the energy, the energy from the potential and contact interaction terms are

$$2\pi \int_0^{2s} \mathrm{d}\rho \, \frac{1}{2} m\Omega_{tr}^2 (1-\gamma^2)\rho^3 \psi(\rho)^2 + \frac{1}{2} b\tilde{g}\psi(\rho)^4 \rho = \frac{N^2 \tilde{g} b}{6\pi s^2} + \frac{2}{3} m N s^2 \Omega_{tr}^2 (1-\gamma^2) \tag{51}$$

The energy from the long-range dipole-dipole interaction is

$$E_{\Phi 2D} = -C_{dd} \int \mathrm{d}\rho \; \mathrm{d}\rho' \, |\psi(\rho)|^2 U(\rho - \rho') |\psi(\rho')|^2 \tag{52}$$

Doing a coordinate transformation to center of mass and relative coordinates in polar coordinates, ρ_{cm} and ρ_{rel} respectively, and also scaling $\rho_{rel} = \rho_s s$, the kernel transforms as $U(\rho - \rho') \to U(\rho_s s)$. The terms from the densities are a bit more involved since it is angular dependent and yields

$$f(\rho_{cm}, \theta_{cm}, \rho_s, \theta_{rel}) = \frac{-8\rho_s^2 \rho_{cm}^2 s^2 \cos(2\theta_{cm} - 2\theta_{rel}) + \rho_s^4 s^4 - 32\rho_s^2 s^4 - 126\rho_{cm}^2 s^2 + 16\rho_{cm}^4 + 256 s^4}{256 s^4} \tag{53}$$

Remembering the factor s^2 from the coordinate transformation the long-range interaction energy can be expressed as

$$E_{\Phi 2D} = -C_{dd} s^2 \left(\frac{2N}{4s^2\pi}\right)^2 \int_0^{2\pi} \mathrm{d}\theta_{cm} \int_0^{2\pi} \mathrm{d}\theta_{rel} \int_0^{2s} \mathrm{d}\rho_{cm} \int_0^4 \mathrm{d}\rho_s \, \rho_s \, \rho_{cm} f(\rho_{cm}, \theta_{cm}, \rho_s, \theta_{rel}) \, U(\rho_s s) \tag{54}$$

Doing the integrals over θ_{cm},θ_{rel} and ρ_{cm} one obtains

$$E_{\Phi 2D} = C_{dd} \left(\frac{2N}{4s^2\pi}\right)^2 \int_0^4 \mathrm{d}\rho_s \, \frac{1}{6}\pi^2 s^4 \rho_s (-64 + 3(-4+\rho_s^2)^2) U(\rho_s s) \tag{55}$$

This integral evaluates to quite an ugly expression, but doing a series expansion around $k = s/a_z \to \infty$ to the lowest order the integral can be approximated as $\frac{224\pi^2 s^4}{3k^2}$. So an approximation of the energy from the long-range dipole-dipole interaction reads

$$E_{\Phi 2D} \approx C_{dd} \left(\frac{2N}{(4s)^2\pi}\right)^2 \frac{1}{2(2\pi)^{3/2} a_z^3} \frac{224\pi^2 s^4}{3k^2} = C_{dd}\sqrt{2} N^2 \frac{1}{\pi^{3/2} a_z} \frac{7}{24 s^2} \tag{56}$$

Lastly, to compute the kinetic energy, one has to take into account how the condensate looks at the boundary, since if one was to naively compute the kinetic energy, it would have the form

$$E_{kin} = -2\pi \int \mathrm{d}\rho \, \rho \, \psi(\rho) \frac{\hbar^2}{2m} \nabla^2 \psi(\rho) \tag{57}$$

which does not converge. Therefore we take from [19] an approximate kinetic energy

$$E_{kin} = \frac{5\hbar^2 N}{2(2s)^2 m} \tag{58}$$

We note that we only take the numerical coefficients of the $1/s^2$ term, and not the full logarithmic dependence on s from [19], and that it is the kinetic energy for a 3D system with an isotropic trap. However, this does not meaningfully impact the calculations, since the interaction terms will dominate, and we simply approximate the kinetic energy for completeness. Thus the full energy for the Thomas-Fermi distribution is

$$E_{\mathrm{TF}} = \frac{5\hbar^2 N}{8s^2 m} + \frac{N^2 \tilde{g} b}{6\pi s^2} + \frac{2}{3} m N s^2 \Omega_{tr}^2 (1-\gamma^2) + C_{dd}\sqrt{2} N^2 \frac{1}{\pi^{3/2} a_z} \frac{7}{24 s^2} \tag{59}$$

Solving for s when minimizing the energy yields the approximation

$$s_{\mathrm{TF}} = \sqrt[4]{\frac{(15/4)\pi\hbar^2 + N m g'_{\mathrm{TF}}}{4\pi m^2 \Omega_{tr}^2 (1-\gamma^2)}} \tag{60}$$

Where

$$g'_{\mathrm{TF}} = b\tilde{g} + \frac{7\sqrt{2} C_{dd}}{4\sqrt{\pi} a_z} \approx 0.46 \frac{g}{a_z} + 1.7 \frac{C_{dd}}{a_z} \tag{61}$$

We must consider that the kinetic term is indeed an approximation, and since we will compare s_{TF} to that of s_{Gauss}, we must make sure that the kinetic energy from the Thomas-Fermi ansatz is larger than that of the Gaussian, since the latter optimizes the kinetic energy. We see that for Dysprosium and Erbium the ratio of the kinetic energies $E_{\mathrm{Gauss,Kin}}/E_{\mathrm{TF,Kin}}$ is 0.54 in both cases, so in this regard the Thomas-Fermi approximation is reasonable.

3.3 Comparison of Gaussian and Thomas-Fermi ansatz

We have treated the quasi-2D description both assuming a Gaussian and Thomas-Fermi distribution for the density, so to determine which is better, we compare the minimized energies. For both Er and Dy the ratio for the energy of the Thomas-Fermi and Gaussian distributions is $E_{\mathrm{TF}}/E_{\mathrm{Gauss}} \approx 0.67$, thus the Thomas-Fermi distribution gives a lower energy, and so is a better solution. These ratios are all independent of γ, so as long as $\gamma < 1$ the Thomas-Fermi distribution is assumed to be the best for our purposes. For the sake of obtaining estimates, we assume that $\omega_z = 2\pi$ kHz, resulting in $a_z = 0.25\mu$m, and that $\omega_x = \omega_y << \omega_z$. The 'dipolar length' of Dy is $a_{\mathrm{ddDy}} = 131\, a_0$ and for Er $a_{\mathrm{ddEr}} = 65.5\, a_0$, where a_0 is the Bohr radius [10]. Furthermore, the scattering length of Dy and Er assumed to be $a_{\mathrm{Dy}} = 91\, a_0$ [10] [12] and $a_{\mathrm{Er}} = 53.8\, a_0$ [10] respectively. To obtain the dipole-dipole interaction strength C_{dd} the relation [18]

$$C_{dd} = \frac{a_{dd} 12\pi\hbar}{m} \tag{62}$$

is used. From this we immediately expect that Dy will perform better at reaching the QH regime, since the dipole-dipole interaction strength is approximately 2 times bigger than that of Er.

We then see whether C_{dd} or g is the dominant interaction strength in both the Gaussian and Thomas-Fermi case. Since

$$g'_{\mathrm{TF}} = \frac{1.7\, C_{dd}}{\sqrt{\frac{\hbar}{m\omega_z}}} + \frac{0.46\, g}{\sqrt{\frac{\hbar}{m\omega_z}}} \tag{63}$$

and

$$g'_{\mathrm{Gauss}} = \frac{1.9\, C_{dd}}{\sqrt{\frac{\hbar}{m\omega_z}}} + \frac{0.46\, g}{\sqrt{\frac{\hbar}{m\omega_z}}} \tag{64}$$

w can find when the C_{dd} term is larger than the g term in each case, which is when $C_{dd}/g > 0.24$ for the Gaussian, and when $C_{dd}/g > 0.27$ for the Thomas-Fermi. Since for Dy and Er we have that

$$\frac{C_{ddDy}}{g_{Dy}} = 6.44 \text{ and } \frac{C_{ddEr}}{g_{Er}} = 3.65, \tag{65}$$

the dipole-dipole contact interaction strength C_{dd} is the dominating parameter in both the Gaussian and Thomas-Fermi ansatz and for each element. We further note that the interaction terms determines the best shape, since the Gaussian has a more peaked center "favoring" a weaker contact interaction, and the Thomas-Fermi distribution is more spread out allowing for a stronger contact interaction, as one can see from Figure 4.

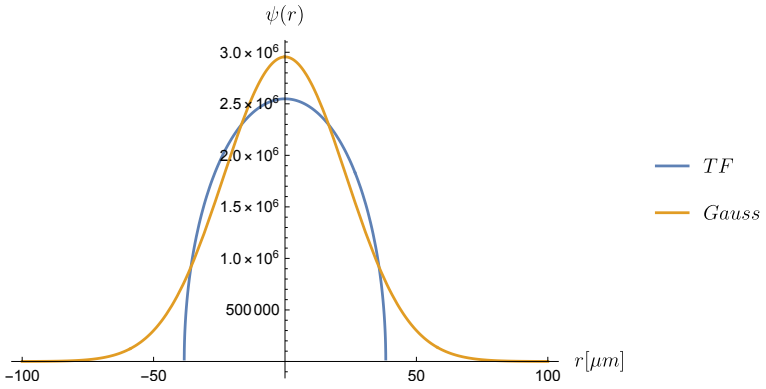

Figure 4: The Gaussian and Thomas-Fermi distribution for Er, at $N = 15000$, $\gamma = 0.99$ and $a_z = 0.25\mu$m. We see that within the Thomas-Fermi radius, the Thomas-Fermi distribution is more spread out and has a lower peak than that of the Gaussian distribution.

4 Reaching the Quantum Hall regime

Since for both the Gaussian and Thomas-Fermi ansatz we see that g' is lager than the bare contact interaction g, we expect that the Quantum Hall regime will be more readily reached [9].

To describe the different phases the condensate goes through, 3 characteristic lengths are introduced, and a phenomenological model is proposed, as in [9]. First, the superfluid healing length $\xi = \hbar/\sqrt{2mng'} \propto 1/(g')^{1/4}$, which describes the length at which the gas recovers its superfluid state from some edge. The magnetic length l_B describing the radius of the synthetic cyclotron motion of a charged particle in a B-field. When $B \to \infty$, $l_B \to 0$ since the cyclotron motion of the charges will be bent more and more, thus making the radius smaller. Lastly, the Lindemann length $l_{\mathrm{L}} \approx 1/\sqrt{\pi n} \propto (g')^{1/4}$, describing the size of the quantum fluctuations that the vortices experience [7]. Together with the Lindemann parameter $\alpha_L \approx 0.4$, these create a criterion for melting, in this case the vortex lattice [20]. When the fluctuations become bigger than the inter-vortex distance, we expect to see the vortex lattice melt.

The phases can be described by the relative sizes of the aforementioned lengths, by seeing what happens when decreasing the magnetic length l_{B}. Starting with the regime $l_{\mathrm{L}}/\alpha_L < \xi/\alpha_\xi < l_{\mathrm{B}}$, we expect to be in a so-called superfluid BEC phase, and depending on how fast the condensate is rotating, a vortex lattice will be present. Increasing the rotation, and thus lowering l_{B}, we will at some point reach the regime $l_{\mathrm{L}}/\alpha_L < l_{\mathrm{B}} < \xi/\alpha_\xi$, where the condensate enters into the LLL vortex lattice . Here $\alpha_\xi = \xi/l_{\mathrm{B}} \approx 0.3$ at the point where the condensate enters the LLL vortex lattice. In the LLL regime it is important to note that the inter-vortex distance scales with the magnetic length l_{B}, thus if the relation $l_{\mathrm{L}}/l_{\mathrm{B}}$ becomes sufficiently large, specifically when reaching α_L, the vortex lattice becomes unstable and melts [7] [9].

When the vortex lattice melts we reach the strongly correlated QH regime where $l_{\mathrm{B}} < l_{\mathrm{L}}/\alpha_L < \xi/\alpha_\xi$ [7], given that $g' < g_o$, where g_o is the optimal contact interaction where the QH regime is

most easily reached.

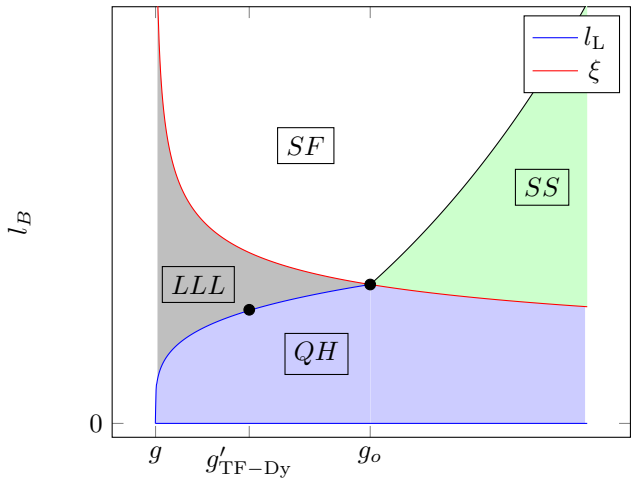

Figure 5: Schematic phase-diagram of BEC. For high l_B we expect to be in a superfluid phase (SF). Increasing l_B the condensate will at some point, assuming $g' < g_o$, enter the LLL regime, which can be suppressed by increasing the contact interaction g'. Further increasing l_B will at some point result in the vortex lattice of the LLL regime to melt, and the condensate enters the QH regime. As we shall see, for large l_{B}, increasing g' the BEC will at some point enter a supersolid (SS) state.

An object that can characterize these different phases is the filling factor

$$\nu = \frac{n}{n_\nu} = \frac{2\pi\hbar n}{B} \tag{66}$$

The ratio of the density of the 2D system n and the areal density of the vortices n_ν. From the definitions of l_{L} and l_{B} we obtain that $\nu \propto (l_{\mathrm{B}}/l_{\mathrm{L}})^2$, meaning that, when ν becomes lower than some critical value the LLL vortex lattice melts and we enter the QH regime [7]. It is clear that ν can be lowered by decreasing the density of the condensate, which we have done by considering the dipole-dipole interaction, or by increasing the synthetic B-field. In this project we will assume that the critical value for the onset of the QH regime is $\nu_{c,o} = 8$, however, it must be noted that other more conservative estimates of $\nu_{c,o}$ are in the range $\nu_{c,o} < 6$, making it harder to reach the QH regime. Therefore an effective Lindemann factor $\alpha'_l = \sqrt{2/\nu_{c,0}}$ is introduced, where $\alpha_l \approx 0.4$ comes from $\nu_{c,0} \approx 8$ [9].

Since the density of the gas is chosen to be $n = N/(4\pi s^2)$ for both the Gaussian and the Thomas-Fermi ansatz, it scales like $1/\sqrt{g'}$. Comparing the bare contact interaction term in g' and the dipole-dipole term, it can be seen how much bigger the interaction g' is compared to g. In the Thomas-Fermi case for Dy and Er g' is a factor of $x_{\mathrm{TF,Dy}} \approx 17$ and $x_{\mathrm{TF,Er}} \approx 14.5$ bigger than g. Thus n and therefore also ν is decreased by a factor of $\mathbf{f}_{\nu,\mathrm{Dy}} \approx 4.1$ and $\mathbf{f}_{\nu,\mathrm{Er}} \approx 3.8$ respectively.

Since the LLL vortex lattice phase is determined by when $\xi/\alpha_\xi > l_L/\alpha_L$, it is clear that the ratio $\xi/l_L \propto 1/\sqrt{g'}$ is decreased by a factor of either $\mathbf{f}_{\nu,\mathrm{Dy}}$ or $\mathbf{f}_{\nu,\mathrm{Er}}$ when the dipole-dipole interaction is incorporated. This suggests that it will be easier to reach the QH regime when working with dipolar gases, as seen in Figure 5.

We can also see that, for some optimal contact interaction g_o the LLL vortex lattice phase is fully suppressed and the QH is optimally reached, specifically when $\xi/\alpha_\xi \approx l_L/\alpha'_L$. From this relation, an optimal value for the effective contact interaction [9] can be expressed as

$$g_o = \frac{\pi\hbar^2}{m\nu_{c,0}\alpha_\xi^2} \tag{67}$$

After g_o the QH phase will be suppressed once again, since the healing length keeps decreasing. It would be an optimal scenario if the effective contact interactions including the dipolar effects where to be greater than g_o, since decreasing the interaction strength is more easily done than the opposite, and so we could reach g_o. However from Table 1 we see that this is not the case, and that g' for both Er and Dy occur before g_o.

	$\frac{g}{\sqrt{2\pi}a_z}[\text{kHz}\cdot\mu\text{m}^2]$	$g'_{\text{Gauss}}[\text{kHz}\cdot\mu\text{m}^2]$	$g'_{\text{TF}}[\text{kHz}\cdot\mu\text{m}^2]$	$g_o[\text{kHz}\cdot\mu\text{m}^2]$	g'_{Gauss}/g_o	g'_{TF}/g_o
Er	$0.0221\hbar$	$0.411\hbar$	$0.371\hbar$	$1.67\hbar$	0.246	0.222
Dy	$0.0376\hbar$	$0.820\hbar$	$0.738\hbar$	$1.69\hbar$	0.485	0.437

Table 1: Comparison of g' in both the Gaussian and Thomas-Fermi case, and the optimal g_o for entering the QH regime for $\omega_z = 2\pi\,\text{kHz}$. In all four cases g' is lower than g_o, but we see that the g' in all cases are bigger then the bare contact interaction g.

For reaching the QH regime given an effective contact interaction g', we determine what γ must be to do so. We will assume a condensate of about $N = 15000$ atoms and that $\omega_z = 2\pi\,\text{kHz}$.

We find an expression for ν to determine for what γ we reach $\nu_{c,0}$. This is done by using the density of the condensate $n = N/(4\pi s^2)$ and the expression for the filling factor Eq. (66), thus obtaining an expression of ν for the Gaussian distribution

$$\nu_{\text{Gauss}} = \frac{N}{4\gamma}\sqrt{\frac{2\pi\hbar^2(1-\gamma^2)}{Nmg' + 2\pi\hbar^2}} \tag{68}$$

And for the Thomas-Fermi distribution, ν is almost the same, only modified by the form of s_{TF}, thus

$$\nu_{\text{TF}} = \frac{N}{4\gamma}\sqrt{\frac{4\pi\hbar^2(1-\gamma^2)}{Nmg' + (15/4)\pi\hbar^2}} \tag{69}$$

In Figure 6 we see that for different choices of γ we can reach $\nu_{c,o}$ for different N. The resulting values for γ at which we reach $\nu_{c,o}$ for 15000 atoms, for both Er and Dy, is given in Table 2. For both Er and Dy, γ has to be close to unity to reach the QH regime, making it unrealistic to achieve in an experimental setting. Lowering N will make it easier to reach the QH regime, so for a system of a 3000 Dy atoms, we need $\gamma \approx 0.975$ to do so.

Element	Gaussian	Thomas-Fermi
Er	$\gamma = 0.994$	$\gamma = 0.997$
Dy	$\gamma = 0.989$	$\gamma = 0.995$

Table 2: Approximate γ for different cases such that $\nu = \nu_{c,o} = 8$ when $N = 15000$ for $\omega_z = 2\pi\,\text{kHz}$.

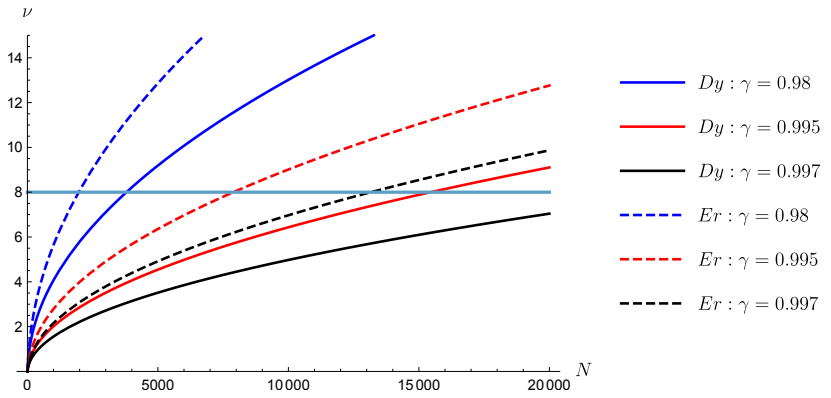

Figure 6: The filling factor for both Er (dashed lines) and Dy (full lines) using the Thomas-Fermi ansatz are plotted for different values of γ, and assuming that $\nu_{c,o} = 8$. For $N = 15000$ we see that we need a $\gamma > 0.995$ for both cases to reach $\nu = 8$, when the frequency along the z-axis is $\omega_z = 2\pi$ kHz.

We see that the best candidate for reaching the QH, between Er and Dy, is Dy. We note that compared to that of Rydberg dressed gases, the reduction in rotation required to enter the QH regime by dipolar interactions is small [9].

Since the QH regime is a strongly correlated phase, the mean-field approach is not valid in this regime, since it discards all correlations. Therefore the GP approach can only be considered to be valid up to the point of the vortex lattice melting, and not beyond. But, as pointed out in [9], the GP approach is expected to be a good description of the LLL vortex lattice near the QH regime.

5 Roton instability

Very recently Norcia et al. [13] have showed that 2D ultra cold atomic dipolar gases can enter a supersolid phase. Supersolidity is a phase where the translational invariance is broken but, as opposed to an ordinary crystal phase, is a coherent state. We want to show that it is realistic to make dipolar systems with $g' \approx g_o$, by using the experimental values that produce a supersolid state and find the interaction needed to enter the supersolid state g_{SS}. We setup a theoretical framework as to approximate for what interactions strength g', for zero rotation, we can enter a supersolid phase, and when this occurs relative to the optimal value g_o to enter the QH regime.

The excitation-spectrum of the condensate is approximated, to estimate when the breakdown of the roton spectrum occurs, signaling the breakdown of translational invariance. To this end, we cannot use the quasi-2D approximation since the roton-instability is not reached within this approximation as shown in [21]. This is because the roton instability appears when the system begins to experience the 3D effects of the sample[14]. Essentially, for the condensate to be in the quasi-2D regime, we expect that $\mu << \hbar\omega_z$, such that the energy per particle is low enough, as to be contained in the ground state of the harmonic trap, but the roton gap appears beyond this limit.

Therefore another approximation is used, where we average out the effects in the z-direction, by assuming that it is a Gaussian distribution along this direction, and also assuming separability of the density. The shape of the Gaussian should be determined by variational methods, since the shape depends on the interactions, but we adopt a distribution $n_z(z) = \frac{1}{a_z\sqrt{\pi}} e^{-z^2/a_z^2}$ which is normalized to 1, where $a_z = \sqrt{\hbar/\omega_z m}$. To make the calculation easier we do them in momentum space, see Appendix B. The terms that we are interested in are the interaction energies from the contact interaction and dipole-dipole interaction. In k-space the Gaussian reads

$$\tilde{n}_z(k_z) = (2\pi)^{-3/2} e^{-\frac{1}{4}k_z^2 a_z^2} \tag{70}$$

and the 3D density distribution in k-space is

$$\tilde{n}(\mathbf{k}) = \tilde{n}_z(k_z)\tilde{n}_{2D}(k_x, k_y) \tag{71}$$

The interaction energy can therefore be expressed as

$$E(\mathbf{k}) = (2\pi)^{3/2} \int dk_x\, dk_y\, dk_z \left[\tilde{U}(\mathbf{k}) + \frac{1}{2}g\right] \tilde{n}_z(k_z)\tilde{n}_z(-k_z)\tilde{n}_{2D}(k_x, k_y)\tilde{n}_{2D}(-k_x, -k_y) \tag{72}$$

From the choice of $\tilde{n}_z(k_z)$ it is clear that $\tilde{n}_z(k_z) = \tilde{n}_z(-k_z)$ and so to integrate out the z-dependence we evaluate

$$(2\pi)^{3/2} \int dk_z \left[\tilde{U}(\mathbf{k}) + \frac{1}{2}g\right] \tilde{n}_z^2(k_z) \tag{73}$$

Resulting in the energy

$$E(\mathbf{k}) = \int dk_x\, dk_y \left[\tilde{U}_{eff}(k_\perp) + \frac{1}{8\sqrt{2}\pi^{5/2}a_z}g\right] \tilde{n}_{2D}(k_x, k_y)\tilde{n}_{2D}(-k_x, -k_y) \tag{74}$$

Where

$$\tilde{U}_{eff}(k_\perp) = \frac{1}{3\pi a_z}C_{dd}\left(1 - \frac{3}{2}\sqrt{\frac{\pi}{2}}e^{\frac{1}{2}k_\perp^2 a_z^2}k_\perp a_z \mathrm{Erfc}\left(\frac{k_\perp a_z}{\sqrt{2}}\right)\right) = \frac{1}{3\pi a_z}C_{dd}h(k_\perp) \tag{75}$$

And $k_\perp^2 = k_x^2 + k_y^2$. We have reduced the problem to being effectively 2D and we see that the dipole-dipole interaction energy is momentum dependent. From Figure 7 we see that for small momenta ($k_\perp a_z < 1$) the shape of the interaction h is repulsive, as we expect in the quasi-2D regime. On the other hand, at larger momenta ($k_\perp a_z > 1$) we see that the interaction energy becomes negative, and thus we have an attractive interaction since the dipoles 'feel' the 3D nature of the condensate.

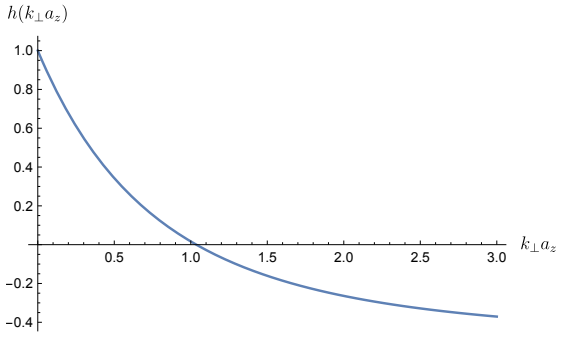

Figure 7: The shape of the interaction as a function of momentum. We see that at $k_\perp a_z \approx 1$ the interaction energy becomes negative, and depending on how big g_{3D} is, this will have an effect on the excitation spectrum. Intuitively, for high enough momentum, the dipoles start to feel the 3D nature of the condensate, which makes the energy from the interaction negative (attractive), instead of purely repulsive, as in the quasi-2D limit.

The goal is to determine the excitation-spectrum of the sample, and this is done by using the Bogoliubov equations, which are obtained by linearizing the variation of the GPE in $\delta\psi$ and $\delta\psi^*$, and demanding that the solution to the equations one obtain in $\delta\psi$ and $\delta\psi^*$ are periodic with time [4]. The generic excitation spectrum obtained by this method is

$$\omega^2 = k^2\left(\frac{\hbar^2 k^2}{4m^2} + \frac{n}{m}U\right) \tag{76}$$

Here U is simply a stand-in for all non-linear $|\psi|^2$ terms in the GPE in momentum space. In other words, the contact and dipole-dipole interactions. In this case

$$U = \tilde{U}_{eff}(k_\perp) + \frac{1}{8\sqrt{2}\pi^{5/2}a_z}g \tag{77}$$

Thus the excitation spectrum with dipole-dipole interaction, assuming a Gaussian distribution along the z-axis is

$$\omega^2 = k_\perp^2\left(\frac{\hbar^2 k_\perp^2}{4m^2} + \frac{n}{m}\left(\frac{1}{8\sqrt{2}\pi^{5/2}a_z}g + \frac{1}{3\pi a_z}C_{dd}h(k_\perp)\right)\right) \tag{78}$$

Rewriting this in units of the frequency of the trap $\omega_z = \frac{\hbar}{a_z^2 m}$, by using that $\omega^2 = \frac{\omega^2}{\omega_z^2}\omega_z^2$ we get

$$\omega^2 = k_\perp^2 a_z^2\left(\frac{a_z^2 k_\perp^2}{4} + \frac{nma_z}{\hbar^2}\frac{1}{8\sqrt{2}\pi^{5/2}a_z}g + g_{3D}h(k_\perp)\right)\omega_z^2 \tag{79}$$

Where we have defined the dimensionless parameter

$$g_{3D} = \frac{mn}{3\pi\hbar^2 a_z}C_{dd} \tag{80}$$

which describes the strength of $h(k_\perp)$. Here the density n should be that of the 2D system that we found to be $n = N/(4\pi s_{\text{Gauss}}^2)$ and for $\gamma = 0$, since we are looking at the non-rotating system.

For large enough values of g_{3D}, the spectrum gives rise to local minimum as seen in Figure 8 called the roton gap, where the excitations are called rotons, which has been experimentally verified [22]. At some large enough value of g_{3D}, the roton gap has a minimum that takes on complex values, as we see in Fig. 8. There is a value of g_{3D} where the minimum of the roton energy is exactly 0, which is the crossing point from a real minimum to a complex one, where the condensate becomes unstable. When this point is crossed, it signals the breakdown of the translational symmetry of the BEC, since now the bosons do not 'know' at which momenta to condense, either at $k_\perp = 0$ or at some $k_{rot} > 0$ where $\omega(k_{rot}) = 0$. Furthermore, if g_{3D} is increased beyond this point, the gap increases and a multitude of values for the momenta can be chosen in the gap, leading to wave functions with different phases that can interfere with each other developing peak and valleys, thus breaking translational invariance.

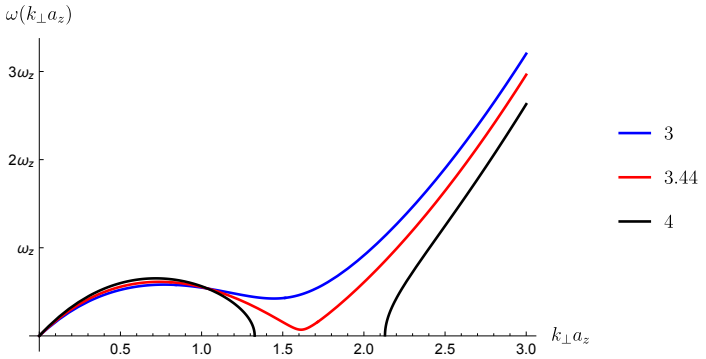

Figure 8: The excitation-spectrum of Dy for different values of g_{3D} for $\gamma = 0$. For large enough values of g_{3D} a second local minimum, called the roton gap appears (blue). At $g_{3D} \approx 3.44$ the minimum of the roton gap result in $\omega = 0$ (red). If g_{3D} gets too large, the roton spectrum breaks down (black).

We stress that this only shows the breaking of translational invariance, and not that the condensate becomes supersolid, but supersolidity is expected to be an intermediate state between a superfluid and crystal phase, as shown in [23].

Finding g_{3D} satisfying a minimum at $k_\perp > 0$ for which $\omega(k_\perp) = 0$ in Eq. (79), can be done numerically, resulting in $g_{3D} \approx 3.44$ [14]. This value has been found when neglecting g, so one could refine the calculation by incorporation the g-term, even though it only has a small contribution.

Using Eq. (80) we can estimate what C_{dd} and thus g' should be to reach the roton instability, by solving for $g_{3D} = 3.44$, and comparing it to the experimental values of g_o for Er and Dy. To make the estimates we use experimental data from [13], and thus set $\omega_z = 167\ 2\pi$Hz, $\omega_x = \omega_y = 33\ 2\pi$Hz and $N = 70000$.

It is important to note that the trapping used in [13] is fully anisotropic, meaning that $\omega_x \neq \omega_y \neq \omega_z$. Taking this anisotrpy into account would in this case lower the interaction strength needed to enter the supersolid phase g_{SS}, since we have chosen $\omega_y = 33\ 2\pi$Hz instead of ω_y in a range $75\,2\pi\,\text{Hz} - 120\,2\pi\,\text{Hz}$ as used in [13]. In Table 3 we see g_{SS} for both Er and Dy occurs after g_o, indicating that $g_{SS} \approx g_o$ can be reached by modifying parameters in Eq. (80) to lower g_{SS}.

Element	g_{SS} [kHz $\cdot\ \mu$m^2]	g_o [kHz $\cdot\ \mu$m^2]	g_{SS}/g_o
Er	$4.85\hbar$	$1.67\hbar$	2.91
Dy	$4.95\hbar$	$1.69\hbar$	2.93

Table 3: Comparing the physical values of g_{SS} for Er and Dy, with the dipole-dipole interaction strengths required to reach the point of roton instability when $\gamma = 0$, and the optimal interaction to most easily reach the QH regime g_o. For both Dy and Er we see that $g_{SS} > g_o$.

These estimates could be further refined by adopting a non-uniform density, by simply using the 2D Thomas-Fermi density

$$n(\rho) = \frac{2N}{(2s)^2\pi}\left(1 - \frac{\rho^2}{(2s)^2}\right) \tag{81}$$

This will however introduce a ρ-dependence to the excitation spectrum, leading to more complex behavior.

6 Conclusion

We have shown that dipolar 2D ultra cold gases, in a combination with rotating traps reduce the filling factor for Dysprosium and Erbium, and thus make it easier to enter the Quantum Hall regime. For a Quantum Hall droplet of 3000 atoms to be reached, the ratio between the rotation and trapping frequency γ for Dysprosium must be $\gamma = 0.975$, being a realistic system to realize. However, to increase the number of atoms one would have to consider γ closer to unity. We also show the the optimal interaction point for entering the Quantum Hall regime is comparable to that of the interaction needed to enter a supersolid state, making reaching the optimal interaction point experimentally feasible.

References

[1] K. B. Davis, M. O. Mewes, M. R. Andrews, N. J. van Druten, D. S. Durfee, D. M. Kurn, and W. Ketterle. Bose-einstein condensation in a gas of sodium atoms. *Phys. Rev. Lett.*, **75**:3969, (1995).

[2] M. H. Anderson, J. R. Ensher, M. R. Matthews, C. E. Wieman, and E. A. Cornell. Observation of bose-einstein condensation in a dilute atomic vapor. *Science*, **269**:198, (1995).

[3] E. A. Cornell and C. E. Wieman. Nobel lecture: Bose-einstein condensation in a dilute gas, the first 70 years and some recent experiments. *Rev. Mod. Phys.*, **74**:875, (2002).

[4] C. J. Pethick and Smith H. *Bose–Einstein Condensation in Dilute Gases*. The Press Syndicate of Cambridge University, The Pitt Building, Trumpington Street, Cambridge, United Kingdom, (2002).

[5] L. Salasnich, A. Parola, and L. Reatto. Effective wave equations for the dynamics of cigar-shaped and disk-shaped bose condensates. *Phys. Rev. A*, **65**:043614, (2002).

[6] A. L. Fetter and A. A. Svidzinsky. Vortices in a trapped dilute bose-einstein condensate. *Journal of Physics: Condensed Matter*, **13**:R135, (2001).

[7] N.R. Cooper. Rapidly rotating atomic gases. *Advances in Physics*, **57**:539, (2008).

[8] A. L. Fetter. Rotating trapped bose-einstein condensates. *Laser Physics*, **18**:1, (2008).

[9] M. Burrello, I. Lesanovsky, and A. Trombettoni. Reaching the quantum hall regime with rotating rydberg-dressed atoms. *Phys. Rev. Research*, **2**:023290, (2020).

[10] L. Chomaz, D. Petter, P. Ilzhöfer, G. Natale, A. Trautmann, C. Politi, G. Durastante, R. M. W. van Bijnen, A. Patscheider, M. Sohmen, M. J. Mark, and F. Ferlaino. Long-lived and transient supersolid behaviors in dipolar quantum gases. *Phys. Rev. X*, **9**:021012, (2019).

[11] L. Tanzi, E. Lucioni, F. Famà, J. Catani, A. Fioretti, C. Gabbanini, R. N. Bisset, L. Santos, and G. Modugno. Observation of a dipolar quantum gas with metastable supersolid properties. *Phys. Rev. Lett.*, **122**:130405, (2019).

[12] F. Böttcher, J. Schmidt, M. Wenzel, J. Hertkorn, M. Guo, T. Langen, and T. Pfau. Transient supersolid properties in an array of dipolar quantum droplets. *Phys. Rev. X*, **9**:011051, (2019).

[13] M. A. Norcia, C. Politi, L. Klaus, E. Poli, M. Sohmen, M.J. Mark, R. Bisset, L. Santos, and F.Ferlaino. Two-dimensional supersolidity in a dipolar quantum gas. arXiv: 2102.05555v1, (2021).

[14] T. Lahaye, C. Menotti, L. Santos, M. Lewenstein, and T. Pfau. The physics of dipolar bosonic quantum gases. *Rep. Prog. Phys.*, **72**:126401, (2006).

[15] D.J. Griffiths and D.J. Schroeter. *Introduction to Quantum Mechanics*. Cambridge University Press, 3 edition, (2018).

[16] T. Ho. Bose-einstein condensates with large number of vortices. *Phys. Rev. Lett.*, **87**:060403, (2001).

[17] W. Bao, Y. Cai, and H. Wang. Efficient numerical methods for computing ground states and dynamics of dipolar bose–einstein condensates. *Journal of Computational Physics*, **229**:7874, (2010).

[18] Y. Cai, M. Rosenkranz, Z. Lei, and W. Bao. Mean-field regime of trapped dipolar bose-einstein condensates in one and two dimensions. *Phys. Rev. A*, **82**:043623, (2010).

[19] F. Dalfovo, G. Pitaevskii, and S. Stringari. The condensate wave function of a trapped atomic gas. *J. Res. Natl. Inst. Stand. Technol.*, **101**:537, (1996).

[20] J. Dietel and H. Kleinert. Lindemann parameters for solid membranes focused on carbon nanotubes. *Phys. Rev. B*, **79**:075412, (2009).

[21] U. R. Fischer. Stability of quasi-two-dimensional bose-einstein condensates with dominant dipole-dipole interactions. *Phys. Rev. A*, **73**:031602, (2006).

[22] D. Petter, G. Natale, R. M. W. van Bijnen, A. Patscheider, M. J. Mark, L. Chomaz, and F. Ferlaino. Probing the roton excitation spectrum of a stable dipolar bose gas. *Phys. Rev. Lett.*, **122**:183401, (2019).

[23] F. Cinti, T. Macrì, W. Lechner, G. Pupillo, and T. Pohl. Defect-induced supersolidity with soft-core bosons. *Nature Communications*, **5**:3235, (2014).

7 Appendix A - Change of variables

The change of variables from eq. (39) to Eq. (40) is done as follows, starting from

$$\langle\psi|\,\Phi_{2D}\,|\psi\rangle = -C_{dd}\frac{N^2}{\pi^2 s^4}\int dx'dy'dx\,dy\,e^{-(x^2+y^2+x'^2+y'^2)/s^2}U(x-x',y-y') \tag{82}$$

Shifting to the center of mass and relative coordinates, $x_{cm} = x + x'/2$ and $x_{rel} = x - x'$ and also for y and y' respectively. The argument of the exponential function can then be written as

$$x^2 + y^2 + x'^2 + y'^2 = (x-x')^2 + 2xx' + (y-y')^2 + 2yy' = x_{rel}^2 + y_{rel}^2 + 2yy' + 2xx' \tag{83}$$

And since $x = x_{cm} + \frac{x_{rel}}{2}$ and $x' = x_{cm} - \frac{x_{rel}}{2}$, with the same for y and y' we get

$$\begin{aligned} &x_{rel}^2 + y_{rel}^2 + 2\left(x_{cm}^2 + y_{cm}^2 - \frac{x_{rel}^2}{4} - \frac{y_{rel}^2}{4}\right) \\ &= 2x_{cm}^2 + 2y_{cm}^2 + \frac{x_{rel}^2}{2} + \frac{y_{rel}^2}{2} \end{aligned} \tag{84}$$

Since the Jacobian is 1 we have

$$-C_{dd}\frac{N^2}{\pi^2 s^4}\int dx_{cm}dy_{cm}dx_{rel}\,dy_{rel}\,e^{-(2x_{cm}^2+2y_{cm}^2)/s^2}e^{-(x_{rel}^2+y_{rel}^2)/2s^2}U(x_{rel},y_{rel}) \tag{85}$$

Now we can go to polar coordinates $r_{cm}^2 = x_{cm}^2 + y_{cm}^2$ and $r_{rel}^2 = x_{rel}^2 + y_{rel}^2$. With no angular dependence we have to remember a factor of $(2\pi)^2$ so one gets

$$\langle\psi|\,\Phi_{2D}\,|\psi\rangle = -C_{dd}\frac{4N^2}{s^4}\int_0^\infty\int_0^\infty dr_{cm}\,dr_{rel}\,e^{-2r_{cm}^2/s^2}e^{-r_{rel}^2/2s^2}U(r_{rel})r_{cm}r_{rel} \tag{86}$$

8 Appendix B - Fourier transformation of energy functional

To find the roton-spectrum we want to represent the energy in momentum space. In other words we want to Fourier transform

$$E_{Int}(\mathbf{r},\mathbf{r}') = \int d\mathbf{r}\,d\mathbf{r}'I(\mathbf{r}-\mathbf{r}')n(\mathbf{r})n(\mathbf{r}') \tag{87}$$

Where we have defined $I(\mathbf{r}-\mathbf{r}')$ as a general interaction, which in this case is

$$I(\mathbf{r}-\mathbf{r}') = \frac{g}{2}\delta(\mathbf{r}-\mathbf{r}') + U(\mathbf{r}-\mathbf{r}') \tag{88}$$

Inserting the inverse Fourier transform of $n(\mathbf{r})$ and $n(\mathbf{r}')$ in 3D, which is

$$n(\mathbf{r}) = \frac{1}{(2\pi)^{3/2}}\int d\mathbf{k}\,e^{i\mathbf{k}\cdot\mathbf{r}}\tilde{n}(\mathbf{k}) \tag{89}$$

So the energy can be expressed as

$$\frac{1}{(2\pi)^3}\int d\mathbf{r}\,d\mathbf{r}'\,d\mathbf{k}\,d\mathbf{k}'\,e^{i\mathbf{k}\cdot\mathbf{r}}e^{i\mathbf{k}'\cdot\mathbf{r}'}I(\mathbf{r}-\mathbf{r}')\tilde{n}(\mathbf{k})\tilde{n}(\mathbf{k}') \tag{90}$$

Changing coordinates to the center of mass and relative coordinates like in Appendix A, with $r' = \rho + \rho'/2$ and $r = \rho - \rho'/2$, one can write

$$\frac{1}{(2\pi)^3}\int d\boldsymbol{\rho}\,d\boldsymbol{\rho}'\,d\mathbf{k}\,d\mathbf{k}'\,e^{i(\mathbf{k}+\mathbf{k}')\cdot\boldsymbol{\rho}}e^{-i(\mathbf{k}-\mathbf{k}')\cdot\boldsymbol{\rho}'/2}I(\boldsymbol{\rho}')\tilde{n}(\mathbf{k})\tilde{n}(\mathbf{k}') \tag{91}$$

$$= \frac{1}{(2\pi)^{3/2}} \int d\boldsymbol{\rho}\, d\mathbf{k}\, d\mathbf{k}'\, e^{i(\mathbf{k}+\mathbf{k}')\cdot\boldsymbol{\rho}} \tilde{I}\left(\frac{\mathbf{k}-\mathbf{k}'}{2}\right) \tilde{n}(\mathbf{k})\tilde{n}(\mathbf{k}') \tag{92}$$

$$= (2\pi)^{3/2} \int d\mathbf{k}\, d\mathbf{k}'\, \delta(\mathbf{k}+\mathbf{k}')\tilde{I}\left(\frac{\mathbf{k}-\mathbf{k}'}{2}\right) \tilde{n}(\mathbf{k})\tilde{n}(\mathbf{k}') \tag{93}$$

So doing the $\mathbf{k}'$ integral, the Dirac delta function dictates the we set $\mathbf{k} = -\mathbf{k}'$, and so we get

$$(2\pi)^{3/2} \int d\mathbf{k}\, \tilde{I}(\mathbf{k})\tilde{n}(\mathbf{k})\tilde{n}(-\mathbf{k}) \tag{94}$$

From [14] it is given that when the bosons are polarized along the z-axis, the Fourier transformation of the interaction is

$$\tilde{I}(\mathbf{k}) = \int d\mathbf{r}\, e^{-i\mathbf{k}\cdot\mathbf{r}} \left(\frac{g}{2}\delta(\mathbf{r}) + U(\mathbf{r})\right)$$

$$= \frac{g}{2} + C_{dd}\left(\frac{k_z^2}{|\mathbf{k}|^2} - \frac{1}{3}\right) \tag{95}$$

Since a Gaussian distribution is assumed along the z-axis, normalized to 1 as

$$n_z(z) = \frac{1}{l\sqrt{\pi}} e^{-z^2/l^2} \tag{96}$$

In momentum space this is still a Gaussian, given as

$$\tilde{n}(k_z) = (2\pi)^{-3/2} e^{-\frac{1}{4}k_z^2 l^2} \tag{97}$$

The densities are in general assumed to be symmetric in k-space, specifically that $\tilde{n}(\mathbf{k}) = \tilde{n}(-\mathbf{k})$, which is evident in the above case.

9 Appendix C - Hamiltonian in rotating frame

Here we transform a Hamiltonian with rotational invariance along the z-axis to a rotating frame, also along the z-axis. We start by acting on the GPE from the left with R, and so

$$-\frac{\hbar}{i}\partial_t\psi = H\psi \tag{98}$$

becomes

$$-R(t)\frac{\hbar}{i}\partial_t\psi = R(t)H\psi \tag{99}$$

$$-R(t)\frac{\hbar}{i}\partial_t\psi = R(t)HR^\dagger(t)R(t)\psi \tag{100}$$

Using that

$$\partial_t\left(R(t)\psi\right) = R(t)\partial_t\psi + \psi\partial_t(R(t)) \tag{101}$$

One obtains

$$-\frac{\hbar}{i}\left(\partial_t\left(R(t)\psi\right) - \partial_t(R(t))\psi\right) = R(t)HR^\dagger(t)R(t)\psi \tag{102}$$

$$-\frac{\hbar}{i}\partial_t\left(R(t)\psi\right) = R(t)HR^\dagger(t)R(t)\psi - \frac{\hbar}{i}\partial_t(R(t))\psi \tag{103}$$

Inserting $R^\dagger(t)R(t) = 1$ between $\partial_t R(t)$ and ψ

$$-\frac{\hbar}{i}\partial_t\left(R(t)\psi\right) = R(t)HR^\dagger(t)R(t)\psi - \frac{\hbar}{i}\partial_t(R(t))R^\dagger(t)R(t)\psi \tag{104}$$

Now rewriting $\tilde{\psi} = R(t)\psi$

$$-\frac{\hbar}{i}\partial_t\tilde{\psi} = R(t)HR^\dagger\tilde{\psi} - \frac{\hbar}{i}\partial_t(R(t))R^\dagger(t)\tilde{\psi} \tag{105}$$

Since the Hamiltonian in the rotating frame has to satisfy $H_{Rot}\tilde{\psi} = -\frac{\hbar}{i}\partial_t\tilde{\psi}$, it must hold that

$$H_{Rot} = R(t)HR^\dagger - \frac{\hbar}{i}\partial_t(R(t))R^\dagger(t) \tag{106}$$

The last term can be easily evaluated using the definition of $R(t)$, so

$$H_{Rot} = R(t)HR^\dagger(t) - \Omega_{rot}L_z \tag{107}$$

$R(t)HR^\dagger(t) = H$ since H has no angular dependence, so the Hamiltonian in the rotating frame is

$$H_{Rot} = H - \Omega_{rot}L_z \tag{108}$$